



Title	High-pressure phase equilibria of tertiary-butylamine hydrates with and without hydrogen
Author(s)	Tanabe, Tomohiro; Sugahara, Takeshi; Kitamura, Kazuma et al.
Citation	Journal of Chemical and Engineering Data. 2015, 60(2), p. 222-227
Version Type	AM
URL	https://hdl.handle.net/11094/91297
rights	This document is the Accepted Manuscript version of a Published Work that appeared in final form in Journal of Chemical and Engineering Data, © American Chemical Society after peer review and technical editing by the publisher. To access the final edited and published work see https://doi.org/10.1021/je5003016 .
Note	

The University of Osaka Institutional Knowledge Archive : OUKA

<https://ir.library.osaka-u.ac.jp/>

The University of Osaka

High-Pressure Phase Equilibria of Tertiary- Butylamine Hydrates with and without Hydrogen

Tomohiro Tanabe, Takeshi Sugahara, Kazuma Kitamura, Takahiro Yamazaki, Takashi
Fujimoto, Kazunari Ohgaki*

Division of Chemical Engineering, Department of Materials Engineering Science, Graduate
School of Engineering Science, Osaka University, 1-3 Machikaneyama, Toyonaka, Osaka 560-
8531, JAPAN

Keyword: Gas hydrate, Phase equilibria, Raman spectroscopy, Tertiary-butylamine, Hydrogen

Thermodynamic stability boundaries of the simple tertiary-butylamine (t-BA) hydrate and t-BA+hydrogen (H₂) mixed hydrate were investigated at a pressure up to approximately 100 MPa. All experimental results from the phase equilibrium measurement, in-situ Raman spectroscopy, and powder X-ray diffraction analysis arrive at the single conclusion that the t-BA hydrates, under pressurization with H₂, are transformed from the structure VI simple t-BA hydrate into the structure II t-BA+H₂ mixed hydrate. The phase transition point on the hydrate stability boundary in the mother aqueous solutions with the t-BA mole fractions (x_{t-BA}) of 0.056 and 0.093 is located at (2.35 MPa, 267.39 K) and (25.3 MPa, 274.19 K), respectively. On the other hand, in the case of the pressurization by decreasing the sample volume instead of supplying H₂, the simple t-BA

hydrate retains the structure VI at pressures up to 112 MPa on the thermodynamic stability boundary.

Introduction

Clathrate hydrates are one kind of inclusion compounds. Guest molecules are enclathrated in cages constructed by hydrogen-bonded water molecules. There are various hydrate structures such as familiar structures I, II, and H. Both the size and shape of the guest molecule mainly determine which structure is formed. In the binary system of H₂ and water, the structure II (sII) hydrate is formed, which constructs of sixteen 5¹²-cages and eight 5¹²6⁴-cages.^{1,2} Adding a particular promoter molecule, the hydrate enclathrating both H₂ and promoter molecules is formed under relatively moderate conditions. For example, the sII H₂+tetrahydrofuran (THF) mixed hydrate is stable at 5 MPa and 279.6 K.³ On the other hand, structure VI hydrate (sVI) is formed only in the case of tertiary-butylamine (t-BA) molecule as a guest species.⁴ The unit cell of sVI hydrate consists of twelve 4⁴5⁴-cages and sixteen 4³5⁹6²7³-cages. The t-BA molecules occupy only 4³5⁹6²7³-cages while all of 4⁴5⁴-cages are vacant. The existence of the distorted and unique cages as well as the possible storage amount of H₂, which is estimated to be the largest among all hydrate structures under some assumptions,⁵ is one of the characteristics of the sVI hydrate. From the characteristics of sVI hydrates, many researchers have studied for sVI hydrates. Kim et al.⁶ and Prasad et al.⁷ reported that the pressurization with CH₄ results in the transformation from the sVI simple t-BA hydrate to the sII CH₄+t-BA mixed hydrate. In addition, Prasad et al.⁸ also reported that the transformation to the sII H₂+t-BA mixed hydrate occurs under the pressurization with H₂, although it is suggested that H₂ molecule ought to occupy the 4⁴5⁴-cage based on the relation between sizes of 4⁴5⁴-cage cavity and H₂ molecule.

These literatures indicate, under pressurization, $5^{12}6^4$ -cage would be more comfortable for the t-BA molecule than $4^35^96^27^3$ -cage. The phase equilibrium relations for the CH_4 +t-BA mixed hydrates with various t-BA concentrations reported by Liang et al.⁹ also support it. According to their results, the thermodynamic stability boundary of the CH_4 +t-BA mixed hydrate at the t-BA composition ($x_{\text{t-BA}}$) of 0.056 is located at a temperature higher than that of $x_{\text{t-BA}} = 0.097$. On the contrary, the isobaric phase equilibrium (temperature - composition) relations for the H_2 +t-BA+water system reported by Du et al.¹⁰ indicate that the maximum equilibrium temperature of H_2 +t-BA mixed hydrates was observed at the vicinity of $x_{\text{t-BA}} = 0.0975$ close to the stoichiometric composition of sVI hydrates ($x_{\text{t-BA}} = 0.093$). The phase equilibrium relations reported by Du et al.¹⁰ exhibit the characteristic behavior as if the sVI H_2 +t-BA mixed hydrate was formed. It implies that H_2 molecules occupy the 4^45^4 -cages of sVI hydrates. However, they claim nothing about the cage occupancy of H_2 .

In general, the structural transition of clathrate hydrates has a significant meaning for practical uses, because the combination ratio of small to large cages drastically varies from hydrate structure to hydrate structure. In addition, the structural transition has further important meanings in H_2 +t-BA mixed hydrate. The sVI H_2 +t-BA mixed hydrate would be a possible H_2 storage medium with the largest storage capacity⁵ if the sVI H_2 +t-BA mixed hydrate were stable at high pressures. It is the purpose of the present study to elucidate the crystal structures of the simple t-BA hydrate and the H_2 +t-BA mixed hydrate under pressurization. We have measured the phase equilibrium relations for the t-BA+water systems with and without H_2 . Based on the phase behavior, Raman spectra, and powder X-ray diffraction (PXRD) profiles, the transformation of sVI t-BA hydrates was discussed.

Experimental Section

The materials used in the present study were summarized in Table 1. All of them were used without further purification.

We used two kinds of high-pressure cells. For the phase equilibrium measurements at a pressure lower than 5 MPa, the pressure-proof glass cell (Taiatsu Techno, HPG-10-1) was used. The detail of the glass cell is given elsewhere^{11,12}. The inner volume and maximum working pressure of the glass cell were 10 cm³ and 5 MPa, respectively. For the phase equilibrium measurements at a pressure higher than 5 MPa and the Raman spectroscopic analysis, we used the high-pressure optical cell with a pair of sapphire windows, which is the same as reported previously.¹³ The thermostated water adjusted by Programming thermocontroller (EYELA NCB-3100) was circulated in the exterior jacket of the high-pressure optical cell. A ruby ball was enclosed into the high-pressure optical cell. The contents were agitated by the ruby ball, which is rolled around by the vibration of vibrator from outside.

The system temperature was measured within an uncertainty of 0.02 K using a thermistor probe (Takara, D-632). The probe was calibrated with a Pt resistance thermometer defined by ITS-90. The system pressure was measured by some pressure gauges (Valcom, VPRT series) according to the working pressures. At a pressure below 1 MPa, from (1 to 10) MPa, from (10 to 100 MPa), and above 100 MPa, an estimated maximum uncertainty is 0.002 MPa, 0.02 MPa, 0.2 MPa, and 0.4 MPa, respectively.

In the t-BA+water binary system, the t-BA aqueous solution prepared at $x_{t-BA} = 0.093$ was introduced into the evacuated high-pressure cell. The content was pressurized up to the desired pressure by the volume change inside the high-pressure cell. After the hydrate formation, the

system temperature was gradually increased (0.1 K step every day) with agitation. When the last particle of hydrates disappeared, the temperature and pressure were measured as the two-phase equilibrium point of the simple t-BA hydrate phase and the aqueous phase with $x_{t\text{-BA}} = 0.093$.

In the H_2 +t-BA+water ternary system, the t-BA aqueous solution prepared at $x_{t\text{-BA}} = 0.056$, 0.075, or 0.093 was introduced into the evacuated high-pressure cell. The content was pressurized with H_2 up to a desired pressure after removing the dissolved air by H_2 pressurization and depressurization. And it was cooled and agitated for the hydrate formation. The subsequent procedure for determining the three-phase (hydrate+aqueous+gas phases) equilibrium point is the same as noted above. Once the hydrate sample for the PXRD measurement was depressurized at 77 K and taken from the cell in the cold room controlled at 263 K, the sample was grained in the mortar immersed in liquid nitrogen. The PXRD pattern was measured at 153 K and atmospheric pressure by use of a diffractometer (Rigaku, model Ultima IV) with a Rigaku D/teX ultra high-speed position sensitive detector and $\text{Cu K}\alpha$ X-ray (40 kV, 50 mA). The PXRD measurements were performed in the stepscan mode with scan rate of $4 \text{ deg} \cdot \text{min}^{-1}$ and step size of 0.02° .

After hydrate crystals were generated by continuous agitation, the system temperature was gradually increased in order to leave a few hydrate crystals. Then it was decreased step by step (0.1 K/hour) to prepare proper-sized hydrate single crystals for Raman spectroscopy. The typical photo of single crystals is shown in Figure 1. The single hydrate crystals were analyzed through a sapphire window by in situ Raman spectroscopy using a laser Raman microprobe spectrophotometer with multichannel CCD detector. The argon ion laser (wavelength: 514.5 nm,

laser spot diameter: 2 μm) was irradiated to the hydrate crystal and the backscatter was taken in with the same lens. The spectral resolution was $\sim 0.7 \text{ cm}^{-1}$.

Results and Discussion

Phase equilibrium relations for the t-BA+water binary system at $x_{\text{t-BA}} = 0.093$ are summarized in Table 2 and shown in Figure 2. The equilibrium temperature of the sVI simple t-BA hydrate at the atmospheric pressure agrees with the literature.¹⁴ The slope (dp/dT) of the phase boundary in the p - T projection seems to be steep at pressures below 10 MPa and gets mild around 20 MPa. To investigate the hydrate structure at a pressure higher than 20 MPa, Raman spectra in the single crystals of the simple t-BA hydrate were measured. Raman spectra in the simple t-BA hydrate are shown in Figure 3. Raman peak corresponding to the intramolecular N–H symmetric stretching vibration mode¹⁵ of t-BA molecule in the sVI simple t-BA hydrate at 0.1 MPa was detected at 3296 cm^{-1} as shown in Figure 3(a). It means that the Raman peak detected at 3296 cm^{-1} is derived from the t-BA molecule enclathrated in the $4^35^96^27^3$ -cage of sVI hydrate. The Raman peak at 3296 cm^{-1} is independent of the pressure and temperature conditions of the present study as shown in Figure 3 (a-e). The present results reveal that no phase transition point exists in the simple t-BA hydrate system with $x_{\text{t-BA}} = 0.093$ at pressures up to 112 MPa.

Phase equilibrium relations for the H_2 +t-BA+water system with $x_{\text{t-BA}} = 0.056$ and 0.093 (on an H_2 -free basis) are summarized in Table 3 and shown in Figure 4. Table 3 includes the data under metastable states. At a glance, both the phase behaviors at $x_{\text{t-BA}} = 0.056$ and 0.093 look similar to that of the sVI simple t-BA hydrate shown in Figure 2. However, unlike in the t-BA+water binary system, some metastable conditions are observed on the extension of both

equilibrium curves of the low-pressure and high-pressure regions. The results indicate the existence of the structural phase transition point. Based on the intersections of both equilibrium curves in the low- and high-pressure regions, the structural phase transition points were located at $\{(2.35\pm 0.05) \text{ MPa}, (267.39\pm 0.03) \text{ K}, x_{\text{t-BA}} = 0.056\}$ and $\{(25.3\pm 0.3) \text{ MPa}, (274.19\pm 0.07) \text{ K}, x_{\text{t-BA}} = 0.093\}$. Comparing the stability boundaries we measured at pressures above the structural transition point, the stability boundary at $x_{\text{t-BA}} = 0.056$ is located at temperatures higher (pressures lower) than that at $x_{\text{t-BA}} = 0.093$. To clarify the trend against the t-BA composition, we also measured the phase equilibrium relations for the H_2 +t-BA+water system with $x_{\text{t-BA}} = 0.075$ (also summarized in Table 3 and shown in Figure 5). The equilibrium curve at $x_{\text{t-BA}} = 0.075$ lies between those of $x_{\text{t-BA}} = 0.056$ and 0.093 . That is, the t-BA composition where the equilibrium temperature of the H_2 +t-BA mixed hydrate becomes the highest under an isobaric condition is 0.056 , which agrees with the stoichiometric composition of sII hydrates. As shown in Figure 5, the hydrate stability boundary we measured in the H_2 +t-BA+water ternary system with $x_{\text{t-BA}} = 0.056$ exhibits different behavior from the reported one¹⁰ with $x_{\text{t-BA}} = 0.0556$. Some metastable decomposition points (listed in Table 3 and plotted by closed rhombuses in Figure S1) of the sVI simple t-BA hydrates we measured at $x_{\text{t-BA}} = 0.056$ appeared to be located on the extension of the reported stability boundary curve¹⁰ at $x_{\text{t-BA}} = 0.0556$ (plotted by open rhombuses in Figure S1). Note that the H_2 molecule, in spite of the H_2 +t-BA+water system, does not occupy the sVI simple t-BA hydrate based on the Raman spectra as stated in next section. This implies that the phase equilibrium data reported in the literature¹⁰ might include the decomposition points of sVI hydrates under metastable state in the datum set under thermodynamically equilibrium conditions.

As shown in Figure 6, the Raman spectra for the H₂+t-BA+water system changed with pressure at both sides of the structural phase transition point. At pressures lower than that of the structural phase transition point (Figure 6(a)-iii and -iv), the Raman peak corresponding to the intramolecular N–H symmetric stretching vibration mode of t-BA molecule was detected at 3296 cm⁻¹, which shows the sVI hydrate formation independent of the t-BA compositions ($x_{t-BA} = 0.056$ and 0.093). At the conditions, the Raman peak derived from H₂ molecules was not observed (Figure 6(b)-iii and -iv and Figure S2 (C)). It means that H₂ molecule does not occupy the 4⁴5⁴-cage of the sVI hydrate in spite of its van der Waals diameter smaller than the void space of 4⁴5⁴-cage. At pressures higher than that of the structural phase transition point (Figure 6(a)-i and -ii), on the other hand, the peak of the t-BA molecule was detected at 3299 cm⁻¹ instead of 3296 cm⁻¹. The 3 cm⁻¹ shift of Raman peak was observed. At the conditions, as shown in Figure 6(b)-i and -ii, the Raman peak corresponding to the H–H stretching vibration of H₂ molecules was detected at 4132 cm⁻¹, which agree well with that in the 5¹²-cages of the sII H₂+THF mixed hydrates¹⁶. The peaks of H₂ rotation modes were also detected (Figure S2 (A) and (B)). PXRD pattern of the H₂+t-BA mixed hydrate prepared at (253 K, 50.8 MPa, $x_{t-BA} = 0.093$) (Figure 7) reveals that the structure of the formed H₂+t-BA mixed hydrate is sII (cubic, *Fd3m*). The obtained lattice constant is $a = (1.751 \pm 0.001)$ nm measured at 153 K. The comparison between the phase equilibrium measurements in the t-BA+water binary and H₂+t-BA+water ternary systems reveals that the transition from sVI hydrate to sII hydrate in H₂+t-BA+water ternary system is caused by the pressurization with H₂ rather than just the compression. The occupancy of H₂ molecules in 4⁴5⁴-cages of the sVI hydrates with H₂ pressurization without structural phase transition is likely to be impossible.

Conclusion

Phase equilibrium relations for the t-BA+water binary system and the H₂+t-BA+water ternary system were measured. No phase transition exists in the t-BA+water binary system on the stability boundary at pressures up to 112 MPa. The phase transition points from the sVI simple t-BA hydrate to the sII H₂+t-BA mixed hydrate are located at (2.35 MPa and 267.39 K) and (25.3 MPa and 274.19 K) in the H₂+t-BA+water system with $x_{t-BA} = 0.056$ and 0.093, respectively. It had been considered that the sVI simple t-BA hydrate would have a pressure-induced structural transition point in a temperature and pressure range of the present study. The present experimental results reveal that the pressurization with small guest species such as H₂ or CH₄, not just the compression, is essential for the phase transition into the sII hydrate from the sVI hydrate.

Table 1. Information on the Chemicals Used in the Present Study.

Chemical Name	Source	Mole Fraction Purity
tertiary-butylamine (t-BA)	Merck, Ltd.	> 0.99
hydrogen (H ₂)	Neriki Gas Co., Ltd.	> 0.999999
water	Wako Pure Chemicals Ind., Ltd.	> 0.9999

Table 2. Phase Equilibrium Data (Pressure p , Temperature T) in the Binary System of t-BA and Water at the t-BA Mole Fraction ($x_{t\text{-BA}}$) of 0.093.^a

T/K	p/MPa
272.13	0.101
273.76	16.2
277.19	33.7
281.11	57.0
284.54	111.7

^a Standard uncertainties u are $u(p) = 0.002$ MPa at $p < 1$ MPa, $u(p) = 0.2$ MPa at $p = (10 \text{ to } 100)$ MPa, $u(p) = 0.4$ MPa at $p > 100$ MPa, and $u(T) = 0.02$ K.

Table 3. Phase Equilibrium Data (Pressure p , Temperature T) in the Ternary System of H₂, t-BA, and Water at the t-BA Mole Fractions ($x_{t\text{-BA}}$) of 0.056, 0.075, and 0.093.^a

T/K	p/MPa	Structure	T/K	p/MPa	Structure
	$x_{t\text{-BA}} = 0.056$			$x_{t\text{-BA}} = 0.075$	
267.30	0.197	VI	269.80	9.11	
267.26	0.493	VI	271.07	12.8	
267.39±0.03 ^b	2.35±0.05 ^b	- ^b	273.80	23.0	
268.03	3.30	II	276.19	34.3	
270.15	8.43	II		$x_{t\text{-BA}} = 0.093$	
271.58	12.8	II	272.48	0.104	VI
273.41	19.7	II	272.48	0.966	VI
274.96	28.1	II	272.59	2.07	VI
277.68	39.9	II	273.37	7.67	VI
281.60	62.3	II	274.12	20.6	VI
285.01	86.4	II	274.19±0.07 ^b	25.3±0.3 ^b	- ^b
267.59 ^c	3.92 ^c	VI ^c	275.91	34.7	II
268.09 ^c	7.12 ^c	VI ^c	279.18	50.4	II
267.03 ^c	1.73 ^c	II ^c	281.83	70.6	II
			284.89	92.0	II
			271.72 ^c	16.3 ^c	II ^c
			272.92 ^c	21.2 ^c	II ^c
			274.02 ^c	25.0 ^c	II ^c

^a Standard uncertainties u are $u(p) = 0.002$ MPa at $p < 1$ MPa, $u(p) = 0.02$ MPa at $p = (1 \text{ to } 10)$ MPa, $u(p) = 0.2$ MPa at $p = (10 \text{ to } 100)$ MPa, and $u(T) = 0.02$ K.

^b Phase transition point determined by the extrapolation of equilibrium curves

^c Metastable states

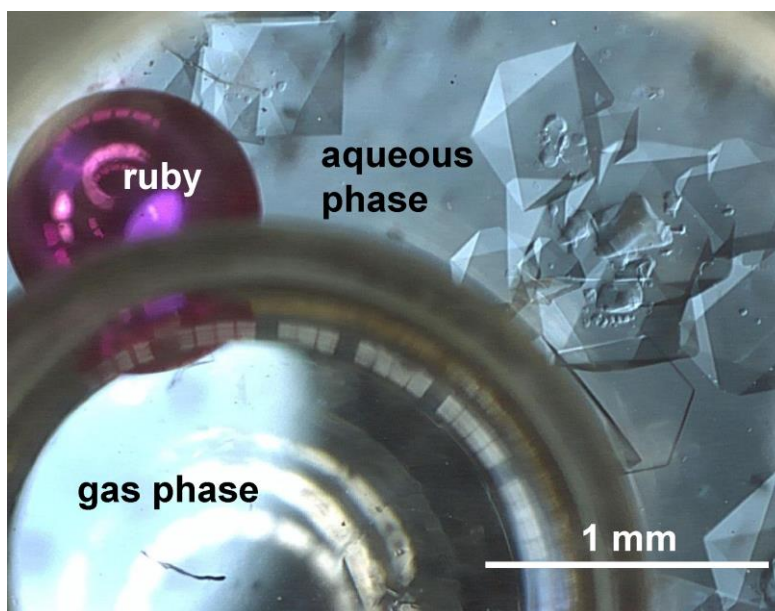


Figure 1. Single crystals of H₂+t-BA mixed hydrate at $x_{t-BA} = 0.093$, $p = 46.1$ MPa, $T = 278$ K.

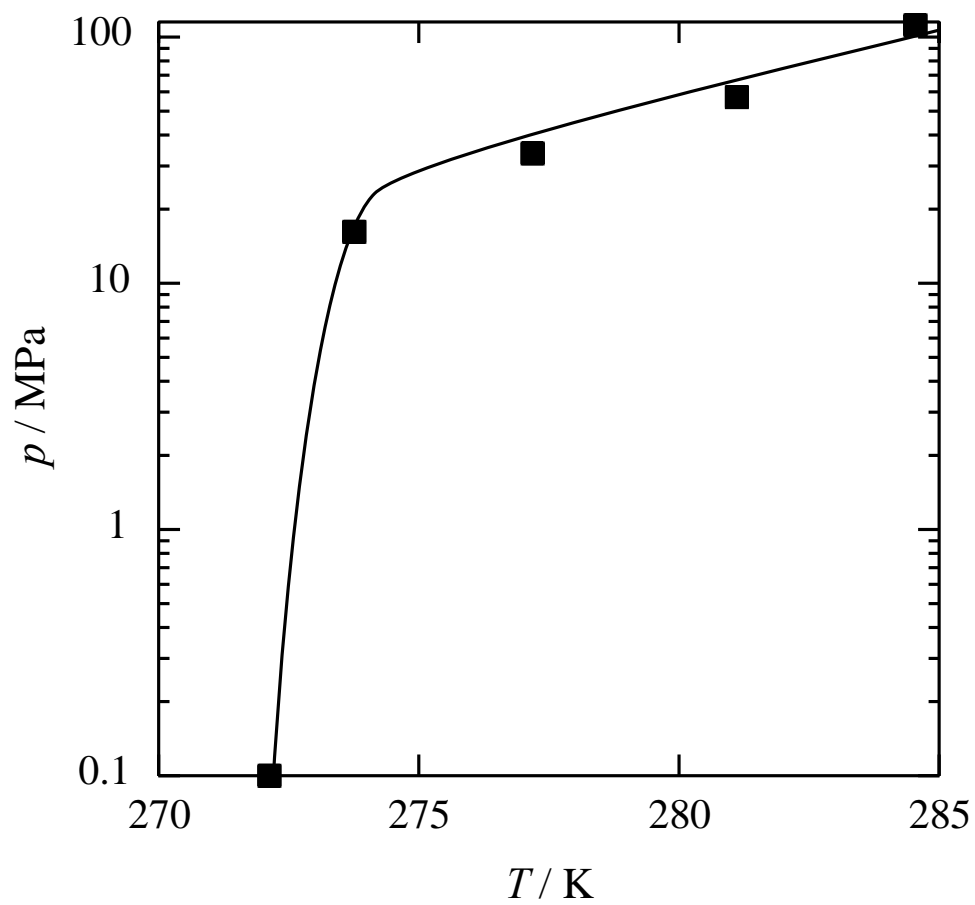


Figure 2. Phase equilibrium relation for the t-BA+water binary system at the t-BA mole fraction of $x_{t-BA} = 0.093$.

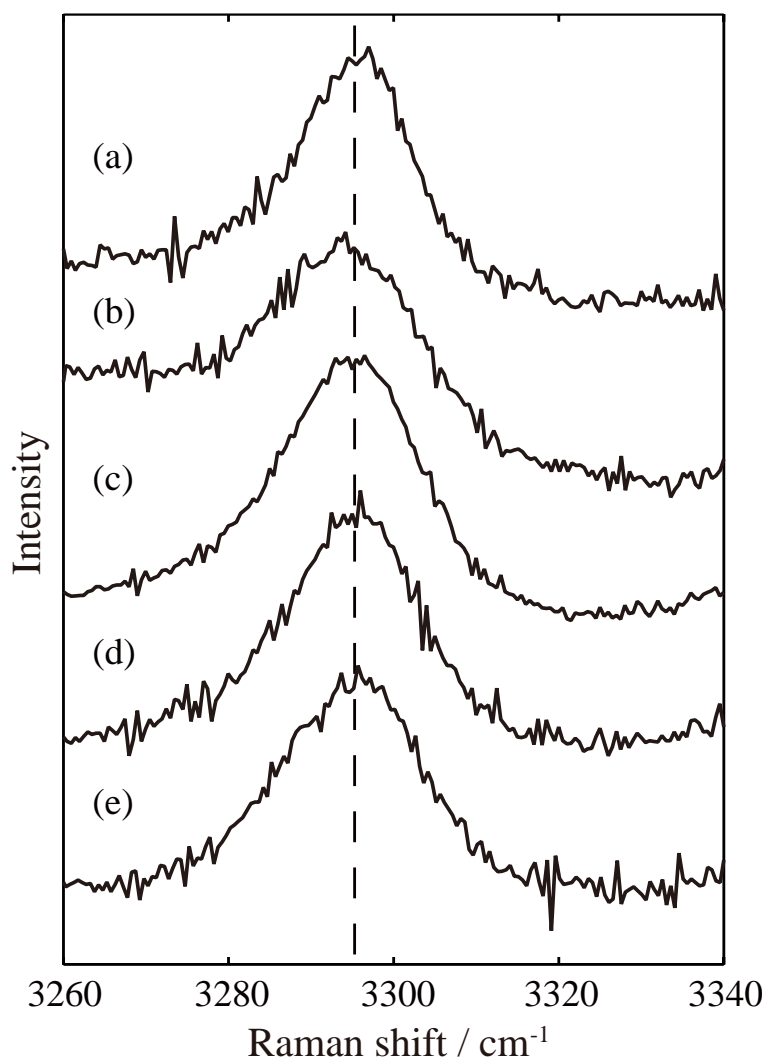


Figure 3. Raman spectra of the intramolecular symmetric N–H vibration mode of the t-BA molecule in the simple t-BA hydrate crystals.

(a): 0.1 MPa, 265 K; (b): 15.2 MPa, 271 K; (c): 25.9 MPa, 274 K; (d): 60.7 MPa, 278 K; (e): 67.9 MPa, 271 K.

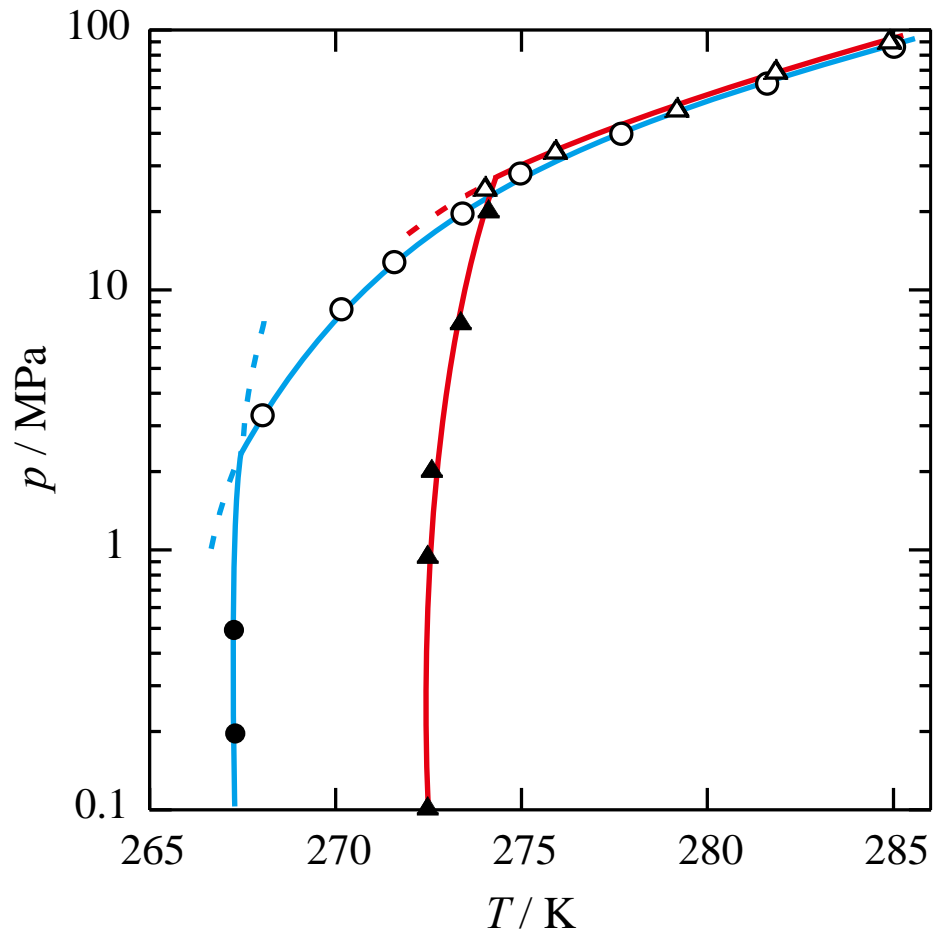


Figure 4. Phase equilibrium relations for the $H_2+t\text{-BA}+\text{water}$ ternary system; open and closed circles: $x_{t\text{-BA}} = 0.056$; open and closed triangles: $x_{t\text{-BA}} = 0.093$. Closed and open keys represent the sVI and sII hydrates, respectively. The solid and dotted lines are fitting lines for the equilibrium data and metastable data observed in the present study, respectively.

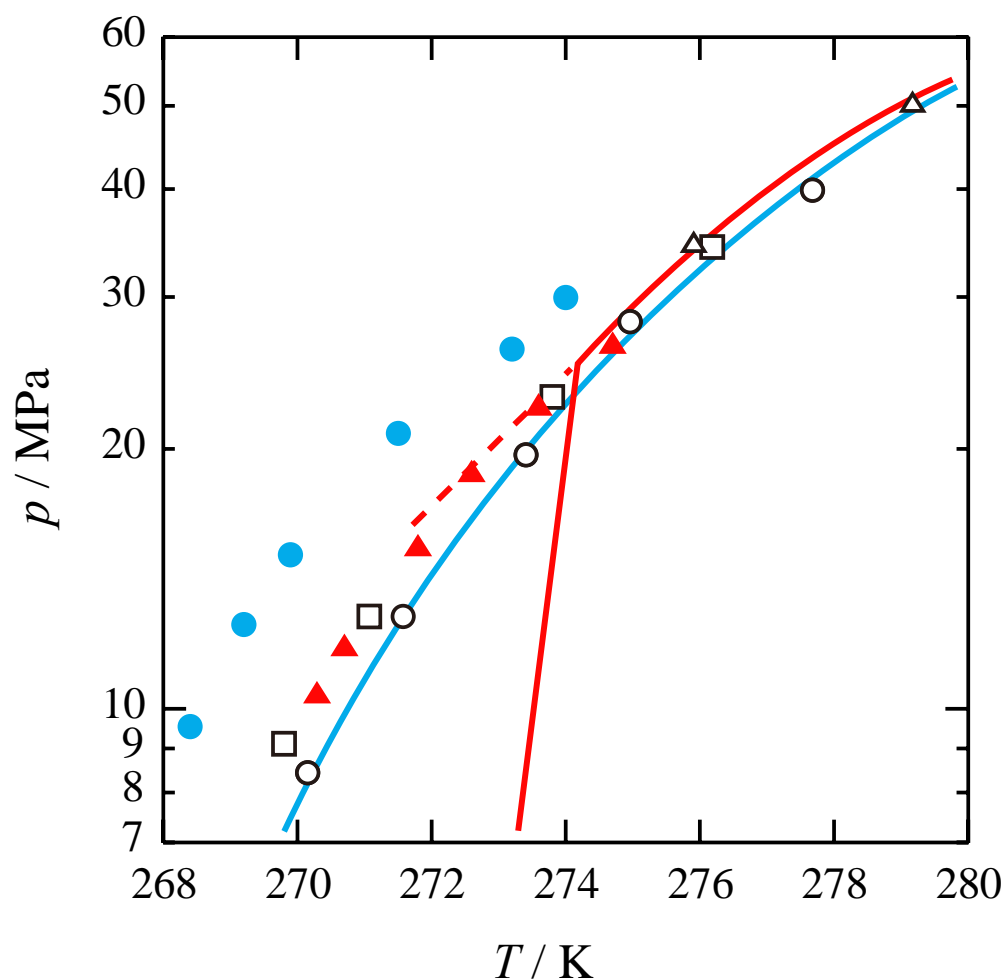


Figure 5. Enlarged phase equilibrium relations for the $\text{H}_2+\text{t-BA}+\text{water}$ ternary system. Open and closed keys represent the results of the present study and the ref.¹⁰, respectively. Open circles: $x_{\text{t-BA}} = 0.056$ (present study); open squares: $x_{\text{t-BA}} = 0.075$ (present study); open triangles: $x_{\text{t-BA}} = 0.093$ (present study); closed circles: $x_{\text{t-BA}} = 0.0556$ (ref.¹⁰); closed triangles: $x_{\text{t-BA}} = 0.0975$ (ref.¹⁰). The solid and dotted lines are fitting lines for the equilibrium data and metastable data observed in the present study, respectively. The equilibrium points (closed triangles in Figure 4) of the sVI hydrates at $x_{\text{t-BA}} = 0.093$ are omitted in this figure.

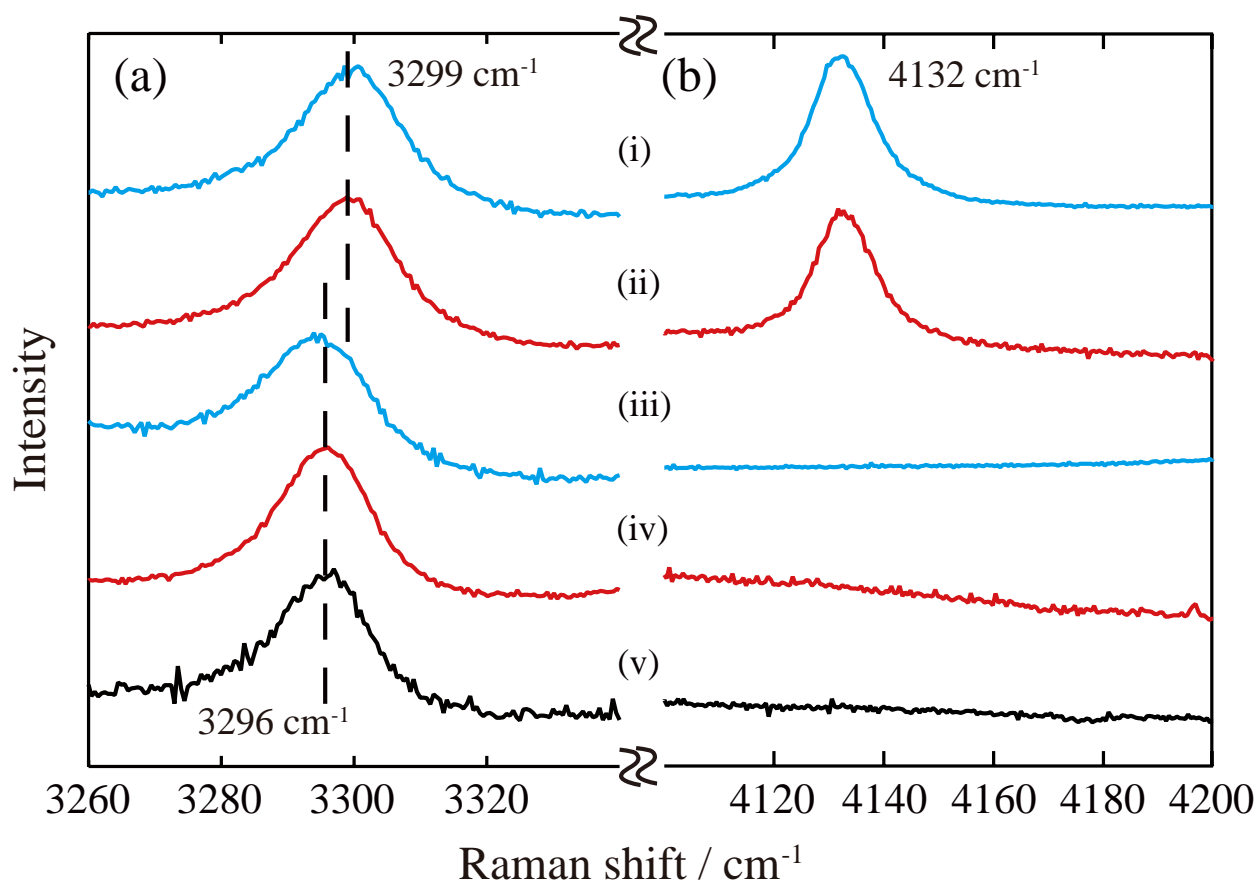


Figure 6. Raman spectra of the intramolecular symmetric N–H vibration mode of the t-BA molecule (a) and the H–H vibration mode of the H₂ molecule (b) in the hydrate crystals prepared from the H₂+t-BA+water ternary system. Blue (i and iii) and red (ii and iv) lines represent $x_{t-BA}=0.056$ and 0.093 , respectively. (i): 40.0 MPa, 277 K; (ii): 46.1 MPa, 278 K; (iii): 1.2 MPa, 266 K; (iv): 20.8 MPa, 274 K. The bottom (v) is the Raman spectrum in the sVI simple t-BA hydrate crystals at 0.1 MPa, 265 K.

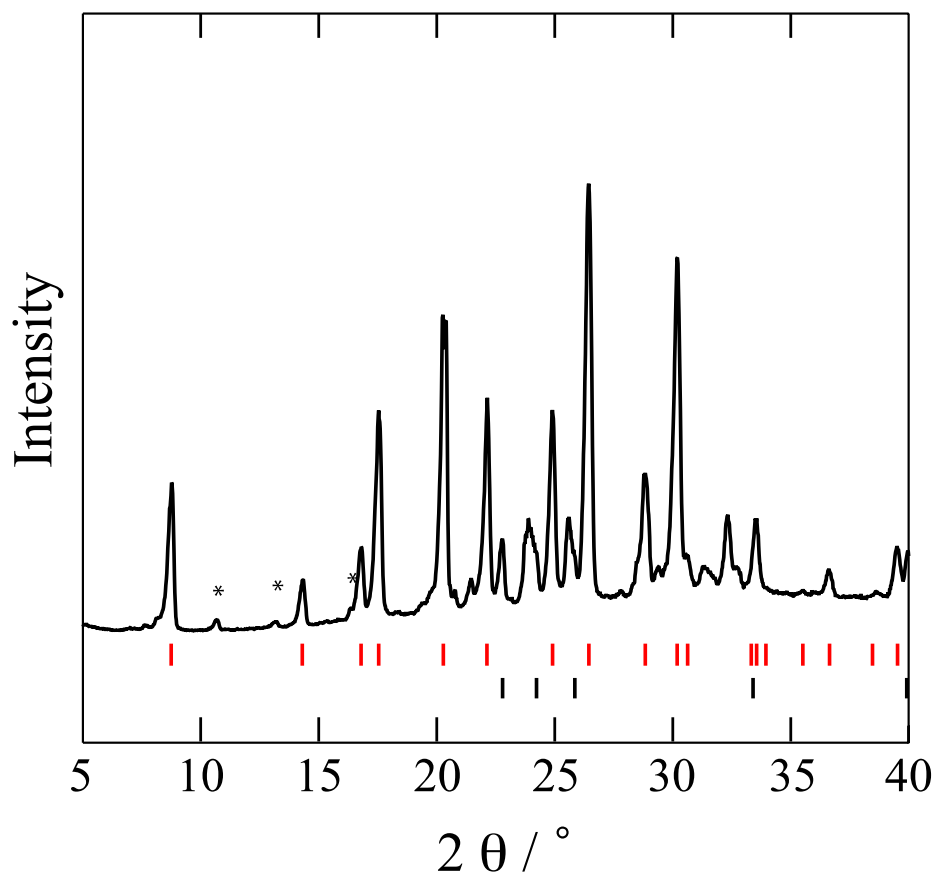


Figure 7. Powder XRD pattern of the sII H₂+t-BA mixed hydrate at $x_{t-BA} = 0.093$, $p = 50.8$ MPa, $T = 253$ K (recorded at 153 K and 0.1 MPa). The vertical bars represent the contribution from sII hydrate (top, red) and ice Ih (bottom, black). Asterisks are derived from the solid t-BA.

AUTHOR INFORMATION

Corresponding Author

* Tel.&Fax.: +81-6-6850-6293. E-mail: sugahara@cheng.es.osaka-u.ac.jp

Notes

The authors declare no competing financial interest.

Supporting Information

Comparison between the phase equilibrium data in the present study and in the reference¹⁰ is shown in Figure S1. Raman spectra of the H₂ rotation modes is shown in Figure S2. This material is available free of charge via the Internet at <http://pubs.acs.org>.

ACKNOWLEDGMENT

We acknowledge financial support from the funding from Advanced Low Carbon Technology Research and Development Program (ALCA) of Japan Science and Technology Agency (JST). We also acknowledge the scientific supports from the “Gas-Hydrate Analyzing System (GHAS)” of the Division of Chemical Engineering, Graduate School of Engineering Science, Osaka University and Rigaku Corporation (for the PXRD measurement at low temperatures). We thank Dr. H. Sato (Osaka University), Dr. Y. Matsumoto (Osaka University), and Mr. K. Nagao (Rigaku Corporation) for the valuable discussion and suggestions.

REFERENCES

(1) Dyadin, Y. A.; Larionov, E. G. ; Aladko, E. Y. ; Manakov, A. Y. ; Zhurko, F. V.; Mikina, T. V.; Komarov, V. Y.; Grachev, E. V. Clathrate formation in water–noble gas (hydrogen) systems at high pressures. *J. Struct. Chem.* **1999**, *40*, 790–794.

(2) Mao, W. L.; Mao, H. K. ; Goncharov, A. F. ; Struzhki, V. V. ; Guo, Q. Z.; Hu, J. Z.; Shu, J. F.; Hemley, R. J. ; Somayazulu, M.; Zhao, Y. Hydrogen Clusters in Clathrate Hydrate. *Science* **2002**, *297*, 2247–2249.

(3) Florusse, L. J.; Peters, C. J. ; Schoonman, J. ; Hester, K. C. ; Koh, C. A.; Dec, S. F.; Marsh, K. N.; Sloan, E. D. Stable Low-Pressure Hydrogen Clusters Stored in a Binary Clathrate Hydrate. *Science* **2004**, *306*, 469–471.

(4) McMullan, R. K.; Jeffrey, G. A. ; Jordan, T. H. Polyhedral Clathrate Hydrates - XIV. The Structure of $(\text{CH}_3)_3\text{CNH}_2 \cdot 9.75\text{H}_2\text{O}$. *J. Chem. Phys.* **1967**, *47*, 1229–1234.

(5) Strobel, T. A.; Koh, C. A. ; Sloan, E. D. ; Hydrogen storage properties of clathrate hydrate materials. *Fluid Phase Equilib.* **2007**, *261*, 382–389.

(6) Kim, D.-Y.; Lee, J.-W. ; Seo, Y.-T. ; Ripmeester, J. A. ; Lee, H. Structural Transition and Tuning of *tert*-Butylamine Hydrate. *Angew. Chem. Int. Ed.* **2005**, *44*, 7749–7752.

(7) Prasad, P. S. R.; Sugahara, T. ; Sloan, E. D. ; Sum, A. K. ; Koh, C. A. Structural Transformations of sVI *tert*-Butylamine Hydrates to sVI Binary Hydrates with Methane. *J. Phys. Chem. A* **2009**, *113*, 11311–11315.

(8) Prasad, P. S. R.; Sugahara, T. ; Sloan, E. D. ; Sum, A. K. ; Koh, C. A. Hydrogen Storage in Double Clathrates with *tert*-Butylamine. *J. Phys. Chem. A* **2009**, *113*, 6540–6543.

- (9) Liang, D.-Q.; Du, J.-W. ; Li, D.-L. Hydrate Equilibrium Data for Methane+*tert*-Butylamine+Water. *J. Chem. Eng. Data* **2010**, *55*, 1039–1041.
- (10) Du, J.-W.; Liang, D.-Q. ; Dai, X.-X. ; Li, D.-L. ; Li, X.-J. Hydrate phase equilibrium for the (hydrogen+*tert*-butylamine+watar) system. *J. Chem. Thermodyn.* **2011**, *43*, 617–621.
- (11) Shimada, N.; Sugahara, K. ; Sugahara, T. ; Ohgaki, K. Phase transition from structure-H to structure-I in the methylcyclohexane+xenon hydrate system. *Fluid Phase Equilib.* **2003**, *205*, 17–23.
- (12) Sugahara, K.; Yoshida, M. ; Sugahara, T. ; Ohgaki, K. Thermodynamic and Raman Spectroscopic Studies on Pressure-Induced Structural Transition of SF₆ Hydrate. *J. Chem. Eng. Data* **2006**, *51*, 301–304.
- (13) Nakano, S.; Moritoki, M. ; Ohgaki, K. High-Pressure Phase Equilibrium and Raman Microprobe Spectroscopic Studies on the CO₂ Hydrate System. *J. Chem. Eng. Data* **1998**, *43*, 807–810.
- (14) Staben, D.; Mootz, D. The 7.25-Hydrate of *tert*-Butylamine. A Semi-Clathrate and Complex Variant of the Cubic 12 Å Structure Type. *J. Inclusion Phenom. Mol. Recognit. Chem.* **1995**, *22*, 145–154.
- (15) Kipkemboi P. K.; Eastal A. J. Vibrational spectroscopic studies of aqueous solutions of *tert*-butyl alcohol and *tert*-butylamine. *Can. J. Chem.* **2002**, *80*, 785–795.

(16) Hashimoto, S.; Sugahara, T. ; Sato, H. ; Ohgaki, K. Thermodynamic Stability of H₂+Tetrahydrofuran Mixed Gas Hydrate in Nonstoichiometric Aqueous Solutions. *J. Chem. Eng. Data* **2007**, 52, 517–520.

TOC

